

Predicting stellar angular diameters from V , I_C , H and K photometry

Arthur D. Adams,^{1★} Tabettha S. Boyajian^{1,2} and Kaspar von Braun³

¹Department of Astronomy, Yale University, 52 Hillhouse Avenue, New Haven, CT 06511, USA

²Department of Physics and Astronomy, Louisiana State University, Nicholson Hall, Tower Drive, Baton Rouge, LA 70803, USA

³Lowell Observatory, 1400 W. Mars Hill Road, Flagstaff, AZ 86001, USA

Accepted 2017 September 11. Received 2017 September 10; in original form 2016 December 13

ABSTRACT

Determining the physical properties of microlensing events depends on having accurate angular sizes of the source star. Using long baseline optical interferometry, we are able to measure the angular sizes of nearby stars with uncertainties ≤ 2 per cent. We present empirically derived relations of angular diameters which are calibrated using both a sample of dwarfs/subgiants and a sample of giant stars. These relations are functions of five colour indices in the visible and near-infrared, and have uncertainties of 1.8–6.5 per cent depending on the colour used. We find that a combined sample of both main-sequence and evolved stars of A–K spectral types is well fitted by a single relation for each colour considered. We find that in the colours considered, metallicity does not play a statistically significant role in predicting stellar size, leading to a means of predicting observed sizes of stars from colour alone.

Key words: stars: early-type – stars: fundamental parameters – stars: general – stars: late-type – planetary systems.

1 INTRODUCTION

Precise stellar radius measurements are important for many sub-fields of astronomy, especially for exoplanet characterization. While precise radii are most readily applicable to transiting exoplanet characterization, they also correspond directly to stellar angular diameters. One notable application for such angular diameters is in constraining the physical properties of microlensing events, for example in distinguishing cases of self-lensing from those of Massive Compact Halo Objects lensing (Calchi Novati et al. 2010; Fukui et al. 2015).

Microlensing systems are often far too distant for direct measurements of the stellar angular size, prompting empirical means to determine stellar sizes from photometry alone.

The surface brightness of a star for a given magnitude is defined in terms of the magnitude and angular diameter (Wesselink 1969; Barnes & Evans 1976; Di Benedetto 2005):

$$S_V = V_0 + 5 \log \theta, \quad (1)$$

where V_0 is an intrinsic magnitude set such that $S_V = V_0$ when the angular diameter $\theta = 1$ mas.

Wesselink (1969) demonstrates a strong empirical correlation between surface brightness and $(B - V)$ colour; a more general correlation between surface brightnesses and colour indices has been shown in Barnes & Evans (1976). Therefore, we expect to be able to construct relations between stellar angular size, colour

and an apparent magnitude from the given colour. Barnes & Evans (1976) further demonstrate that surface brightness is independent of stellar luminosity class, which implies that such an angular size–colour–magnitude relation should hold regardless of whether stars have evolved off the main sequence. Di Benedetto (2005) proposed, through a comparison of the empirical relations for both dwarf and giant stars, that there was enough overlap in the then available data to motivate a combined fit across evolutionary stages.

One photometric magnitude of each colour is used as a baseline for developing a zero-magnitude diameter, the angular diameter each star would appear to have if its apparent magnitude were zero in a selected band:

$$\log \theta_{Q=0} = \log \theta_{LD} + 0.2Q, \quad (2)$$

where θ_{LD} is the angular diameter after correction for limb-darkening and Q is the magnitude in a given band. We construct our relations as polynomials in colour. For a given colour $(P - Q)$

$$\log \theta_{Q=0} = \sum_{n=0}^N c_n (P - Q)^n, \quad (3)$$

where N is an arbitrary order, taken to be the greatest statistically significant order when fitting the data. Determination of angular sizes from observed colours is insensitive to wavelength-dependent extinction for the precisions attainable through this analysis (Barnes & Evans 1976); therefore we neglect extinction correction.

The use of interferometry to measure the angular diameters of stars has played a major role in empirically constraining the radii of nearby stars. Our new relations benefit from recent precise angular diameter measurements of both main-sequence and evolved stars

* E-mail: arthur.adams@yale.edu

using optical interferometry. They extend the results of Boyajian, van Belle & von Braun (2014) with new data and more precise relations for both main-sequence and evolved stars, constructed for a more limited range of spectral types.

Section 2 describes the criteria for data selection and sources of angular diameters and photometry, and the methodology for fitting the data is presented in Section 3. We analyse the results in Section 4, including a comparison with previous works (Section 4.1).

2 DATA

We compile a list of stars with both V , I_C , H and/or K magnitudes and precise angular diameters in Tables 1 and 2. A total of 57 distinct main-sequence stars are selected among all relations, with effective temperatures of 3927–9553 K (spectral types A1–M0), a mean angular diameter uncertainty of 0.013 mas and apparent V magnitudes of 0.03–7.70. The evolved sample contains 50 stars with effective temperatures of 3972–10 330 K (spectral types A1–M0), a mean angular diameter uncertainty of 0.043 mas and apparent V magnitudes of 1.16–6.18. The following subsections outline both the source information as well as selection and classification criteria.

2.1 Stellar classification

We restrict included stars to an effective temperature range of $3900 < T < 10\,500$ K, which approximately captures spectral types A–K.

Evolved stars are selected not based on their listed spectral classes, but by a stellar radius cut of $6 < R_*/R_\odot < 100$. This is done in an attempt to disambiguate the luminosity classes of stars which might have inconsistent classifications in the boundary between subgiants and giants.

Some stars in our sample are known to be in multiple star systems. The presence of additional stars can introduce an offset in flux and visibility of the target star. We adopt the selection precedent from Boyajian et al. (2008); we exclude any binary systems where a secondary star is both separated from the target by at most 5 arcsec and is within 3 mag of the target in any bands used in the analysis.

2.2 Angular diameters

All stars are required to have limb-darkened angular diameters with mean random errors ≤ 2 per cent, and must have been observed on at least two separate occasions. The measurements come from a variety of sources, which are detailed in Boyajian et al. (2012b) and Boyajian et al. (2013) and listed for reference in Tables 1 and 2. Stars with inconsistent diameters (here defined as any two sources differing by at least three times the maximum uncertainty of any measurement) were excluded. We take the uncertainty-weighted means of the remaining measurements for our quoted angular diameters. Angular diameter source instruments include the Palomar Testbed Interferometer, the Very Large Telescope Interferometer, the Sydney University Stellar Interferometer, the Narrabri Stellar Intensity Interferometer, the Mark III interferometer, the Navy Prototype Optical Interferometer and especially the CHARA Array.

2.3 Magnitudes

2MASS photometry (Cutri et al. 2003) is saturated for most of the stars in our sample due to brightness. Therefore, we rely on

earlier photometric catalogues for reliable magnitudes. All magnitudes used are listed in Tables 1 and 2. For the I magnitudes, we use Cousins I_C photometry converted from Johnson I_J sources (Mallama 2014), as well as magnitudes from Koen et al. (2010) for our reddest stars. We use Gezari et al. (1999) for H magnitudes, querying the catalogue for all magnitude measurements centred at $1.65\ \mu\text{m}$. Here, errors of 0.05 mag are assumed as a conservative estimate. The K magnitudes are taken from a combination of Neugebauer & Leighton (1969), Kidger & Martín-Luis (2003) and Kimeswenger et al. (2004). Since the filter profiles for the magnitudes in these catalogues differ appreciably, we choose to convert all into the 2MASS system. Neugebauer & Leighton (1969) magnitudes are originally in the California Institute of Technology (CIT) system (Iyengar et al. 1982), and the Kimeswenger et al. (2004) are listed as Deep Near-Infrared Survey (of the Southern sky) (DENIS) K_S magnitudes. Carpenter (2001) provides transformations from both the CIT and DENIS systems into the 2MASS system (with updated transformations available on the 2MASS website). For the Kidger & Martín-Luis (2003) magnitudes, we first transform into an intermediate system, the Koornneef system (Koornneef 1983). Kidger & Martín-Luis (2003) compare their photometry to the system described in (Koornneef 1983) and find a constant offset in magnitude. From this, we convert to 2MASS via the relation in Carpenter (2001). While significant colour dependence exists for the DENIS and Koornneef transformations, the CIT transformation exhibits only a very weak colour dependence. In light of this, and the lack of accompanying J magnitudes for the Neugebauer & Leighton (1969) K magnitudes, we choose to neglect the colour term, incorporating the error from this omission into our final uncertainty propagation.

In order to calculate colour indices, all stars must have at least one available magnitude in any of the I_C , H and K bands. We exclude stars with inconsistent magnitudes, i.e. magnitudes from different sources whose values disagree by at least triple the largest uncertainty of any one value. The listed uncertainties in the resulting colours are propagated from both the uncertainties from conversion as well as assumed 0.02 mag errors in the original Johnson V magnitudes (Mallama 2014).

3 FITTING PROCEDURE

We choose to construct relations for $V - I_C$, $V - H$, $V - K$, $I_C - H$ and $I_C - K$ (Fig. 1). We start with a constant-only fit of $\log \theta_{Q=0}$ and add polynomial terms in colour, following the form of equation (3). The fitting procedure uses a Levenberg–Markquardt least-squares algorithm provided by the MINPACK-1 Least Squares Fitting routine (Markwardt 2009). For each solution, we perform an F-test (Press et al. 1992) to determine whether the improvement to the relation by adding a polynomial term is statistically significant. Once the functional form is obtained, we run a Monte Carlo simulation by generating 10^4 simulated data sets, randomly choosing colours and diameters drawn from Gaussian probability distributions of each star’s true colour and diameter. The means and standard deviations are given by the initial fit coefficients and their associated uncertainties, respectively. This allows us to incorporate all measurement uncertainties into the relation.

4 ANALYSIS

For each colour, we construct independent fits of unevolved and evolved stars (Fig. 1). Table 3 shows the number of stars, range

Table 1. Selected stellar properties – dwarfs.

HIP	Sp. Type	θ_{LD} (mas)	V	I_C	H	K	θ_{LD} Ref.
3765	K2.5V	0.868 ± 0.004	5.740	4.780 ± 0.027	–	–	1
3821	F9V	1.623 ± 0.004	3.460	–	2.020 ± 0.050	1.821 ± 0.060	2
4151	F9V	0.865 ± 0.010	4.800	4.210 ± 0.027	3.560 ± 0.050	–	2
4436	A6V	0.708 ± 0.013	3.860	3.700 ± 0.027	3.370 ± 0.060	3.365 ± 0.071	3
5336	K1V Fe-2	0.972 ± 0.009	5.170	4.360 ± 0.027	–	–	4
7513	F9V	1.143 ± 0.010	4.100	3.500 ± 0.027	2.990 ± 0.050	2.841 ± 0.080	5, 6
7981	K1V	1.000 ± 0.004	5.240	4.360 ± 0.027	3.345 ± 0.050	–	7
8102	G8.5V	2.080 ± 0.030	3.490	2.630 ± 0.027	1.727 ± 0.050	1.631 ± 0.060	8
12 114	K3V	1.030 ± 0.007	5.790	4.740 ± 0.027	3.542 ± 0.050	–	1
12 777	F7V	1.103 ± 0.009	4.100	3.530 ± 0.027	3.070 ± 0.050	2.761 ± 0.090	2
16 537	K2V (k)	2.126 ± 0.014	3.720	–	1.749 ± 0.050	1.601 ± 0.060	9
16 852	F9IV-V	1.081 ± 0.014	4.290	3.640 ± 0.027	–	2.871 ± 0.100	2
19 849	K0.5V	1.446 ± 0.022	4.430	3.530 ± 0.027	–	–	1, 10
22 449	F6IV-V	1.419 ± 0.027	3.190	2.650 ± 0.027	2.148 ± 0.050	2.031 ± 0.060	11, 2
24 813	G1V	0.981 ± 0.015	4.690	4.040 ± 0.027	3.330 ± 0.050	3.255 ± 0.045	2
27 435	G2V	0.572 ± 0.009	5.970	–	4.499 ± 0.050	–	7
27 913	G0V CH-0.3	1.051 ± 0.009	4.390	–	3.050 ± 0.050	2.971 ± 0.070	2
32 349	A0mA1Va	5.959 ± 0.059	–1.440	–1.430 ± 0.027	–1.387 ± 0.050	–	12, 13, 14, 15, 16
32 362	F5IV-V	1.401 ± 0.009	3.350	2.870 ± 0.027	–	2.111 ± 0.060	2
35 350	A3V	0.835 ± 0.013	3.580	3.450 ± 0.027	–	–	2
36 366	F1V	0.853 ± 0.014	4.160	3.780 ± 0.027	–	–	2
37 279	F5IV-V	5.434 ± 0.050	0.400	–0.140 ± 0.027	–0.569 ± 0.050	–0.669 ± 0.051	13, 17, 18, 19
40 843	F6V	0.706 ± 0.013	5.130	–	3.940 ± 0.050	–	7
43 587	K0IV-V	0.711 ± 0.004	5.960	–	4.140 ± 0.050	–	20
45 343	M0.0V	0.871 ± 0.015	7.640	–	4.253 ± 0.050	–	1
46 733	F0V	1.133 ± 0.009	3.650	3.270 ± 0.027	–	2.711 ± 0.090	2
46 853	F7V	1.632 ± 0.005	3.170	2.610 ± 0.027	2.025 ± 0.050	1.951 ± 0.070	2
47 080	G8IV	0.821 ± 0.013	5.400	–	3.770 ± 0.050	–	2
51 459	F8V	0.794 ± 0.014	4.820	4.240 ± 0.027	–	–	2
53 910	A1IVspSr	1.149 ± 0.014	2.340	2.380 ± 0.027	–	2.361 ± 0.060	2
56 997	G8V	0.910 ± 0.009	5.310	4.580 ± 0.027	–	–	2
57 757	F8.5IV-V	1.431 ± 0.006	3.590	3.000 ± 0.027	2.345 ± 0.050	2.301 ± 0.060	2
57 939	G8. V P	0.686 ± 0.006	6.420	5.570 ± 0.027	–	–	2, 21
64 394	G0V	1.127 ± 0.011	4.230	3.620 ± 0.027	2.923 ± 0.050	2.851 ± 0.100	2
64 924	G7V	1.073 ± 0.005	4.740	3.990 ± 0.027	–	–	22
65 721	G5V	1.010 ± 0.020	4.970	4.190 ± 0.027	3.320 ± 0.050	–	5
66 249	A2Van	0.852 ± 0.009	3.380	3.280 ± 0.027	3.050 ± 0.050	–	2
67 927	G0IV	2.252 ± 0.036	2.680	2.080 ± 0.027	1.390 ± 0.050	1.291 ± 0.051	13, 18, 23, 24
71 284	F4Vkf2mF1	0.841 ± 0.013	4.470	4.020 ± 0.027	3.516 ± 0.050	–	2
72 567	F9IV-V	0.569 ± 0.011	5.860	–	4.530 ± 0.050	–	7
72 659	G7V	1.196 ± 0.014	4.540	–	3.000 ± 0.050	2.651 ± 0.080	2
78 459	G0V	0.735 ± 0.014	5.390	–	3.945 ± 0.050	3.901 ± 0.045	22
81 300	K0V (k)	0.724 ± 0.011	5.770	–	3.910 ± 0.050	–	1
91 262	A1V	3.280 ± 0.010	0.030	0.080 ± 0.027	0.004 ± 0.050	–0.079 ± 0.060	13, 16, 25, 26, 27
92 043	F5.5IV-V	1.000 ± 0.006	4.190	3.660 ± 0.027	–	2.941 ± 0.090	2
93 747	A1V	0.895 ± 0.017	2.990	2.990 ± 0.027	–	2.921 ± 0.080	2
96 100	G9V	1.254 ± 0.012	4.670	3.850 ± 0.027	–	2.811 ± 0.080	4
96 441	F3+ V	0.844 ± 0.009	4.490	4.020 ± 0.027	–	–	2, 6
96 895	G1.5V	0.554 ± 0.011	5.990	5.440 ± 0.027	4.731 ± 0.050	4.569 ± 0.045	7
98 505	K2V	0.385 ± 0.006	7.670	6.680 ± 0.008	–	–	28
102 422	K0IV	2.650 ± 0.040	3.410	2.510 ± 0.027	–	1.201 ± 0.051	29
108 870	K5V	1.881 ± 0.017	4.690	3.530 ± 0.027	–	–	10
112 447	F6V	1.091 ± 0.008	4.200	3.590 ± 0.027	–	2.851 ± 0.080	2
113 368	A4V	2.230 ± 0.020	1.170	1.090 ± 0.027	1.054 ± 0.050	0.981 ± 0.051	19
114 570	F1V	0.648 ± 0.008	4.530	4.160 ± 0.027	–	–	3
114 622	K3V	1.106 ± 0.007	5.570	4.470 ± 0.027	3.400 ± 0.050	–	1
116 771	F7V	1.082 ± 0.009	4.130	3.520 ± 0.027	–	2.731 ± 0.080	2
120 005	K7.0V	0.856 ± 0.016	7.700	–	4.253 ± 0.050	–	1

Angular Diameter References: (1) Boyajian et al. (2012b); (2) Boyajian et al. (2012a); (3) Maestro et al. (2013); (4) Boyajian et al. (2008); (5) Baines et al. (2008); (6) Ligi et al. (2012); (7) Boyajian et al. (2013); (8) Di Folco et al. (2004); (9) di Folco et al. (2007); (10) Demory et al. (2009); (11) van Belle, Creech-Eakman & Hart (2009); (12) Davis & Tango (1986); (13) Mozurkewich et al. (2003); (14) Kervella et al. (2003); (15) Davis et al. (2011); (16) Hanbury Brown et al. (1974); (17) Chiavassa et al. (2012); (18) Nordgren, Sudol & Mozurkewich (2001); (19) Kervella et al. (2004a); (20) von Braun et al. (2011); (21) Crepp et al. (2012); (22) von Braun et al. (2014); (23) van Leeuwen (2007); (24) Thévenin et al. (2005); (25) Ciardi et al. (2001); (26) Aufdenberg et al. (2006); (27) Monnier et al. (2012); (28) Boyajian et al. (2015); (29) Nordgren et al. (1999). **Colour Magnitude References:** Neugebauer & Leighton (1969); Gezari, Pitts & Schmitz (1999); Carpenter (2001); Kidger & Martín-Luis (2003); Kimeswenger et al. (2004); Koen et al. (2010) and Mallama (2014); see Section 2 for more details.

MNRAS **473**, 3608–3614 (2018)

Table 2. Selected stellar properties – giants.

HIP	Sp. Type	θ_{LD} (mas)	V	I_C	H	K	θ_{LD} Ref.
3092	K3III	4.168 ± 0.047	3.270	2.040 ± 0.027	0.551 ± 0.050	0.421 ± 0.051	1, 2
7607	K3- III CN0.5	3.760 ± 0.070	3.590	2.310 ± 0.027	–	0.771 ± 0.041	3
7884	K2/3 III	2.810 ± 0.030	4.450	3.050 ± 0.027	1.409 ± 0.050	1.241 ± 0.031	3
9884	K1IIIb	6.847 ± 0.071	2.010	0.860 ± 0.027	–0.558 ± 0.050	–0.649 ± 0.051	1, 2, 3, 4
13 328	K5.5III	4.060 ± 0.040	4.560	2.820 ± 0.027	–	0.721 ± 0.051	1
20 205	G9.5IIIab CN0.5	2.520 ± 0.030	3.650	–	1.500 ± 0.050	1.481 ± 0.041	5
20 455	G9.5III CN0.5	2.302 ± 0.040	3.770	–	–	1.581 ± 0.051	1, 2, 5
20 885	G9III Fe-0.5	2.310 ± 0.040	3.840	–	–	1.621 ± 0.060	5
20 889	G9.5III CN0.5	2.572 ± 0.046	3.530	–	–	1.291 ± 0.051	1, 2, 5, 6
21 421	K5III	20.297 ± 0.384	0.870	–	–2.653 ± 0.050	–	1, 4, 7, 8
22 453	K3+ III	2.727 ± 0.013	4.890	–	–	1.441 ± 0.041	9
37 826	G9III	8.177 ± 0.130	1.160	0.160 ± 0.027	–1.003 ± 0.050	–1.139 ± 0.051	1, 10, 11, 2, 4
42 527	K1+ III	2.225 ± 0.020	4.590	3.420 ± 0.027	1.941 ± 0.009	1.901 ± 0.070	12
45 860	K6III	8.025 ± 0.142	3.140	1.460 ± 0.027	–0.475 ± 0.050	–0.699 ± 0.031	1, 11, 13, 2
46 390	K3IIIa	9.700 ± 0.100	1.990	0.550 ± 0.027	–1.074 ± 0.050	–1.379 ± 0.060	1
49 637	K3.5IIIb Fe-1:	3.330 ± 0.040	4.390	2.890 ± 0.027	1.190 ± 0.050	1.011 ± 0.070	3
53 229	K0+ III-IV	2.540 ± 0.030	3.790	2.770 ± 0.027	–	1.351 ± 0.041	3
54 539	K1III	4.107 ± 0.053	3.000	1.920 ± 0.027	0.539 ± 0.010	0.371 ± 0.041	1, 2
55 219	K0IV	4.745 ± 0.060	3.490	2.110 ± 0.027	0.415 ± 0.010	0.251 ± 0.041	1, 2
56 343	G7III	2.386 ± 0.021	3.540	2.620 ± 0.027	1.577 ± 0.050	1.491 ± 0.060	14
57 399	K0.5IIIb:	3.230 ± 0.020	3.690	2.580 ± 0.027	1.020 ± 0.050	0.901 ± 0.031	3
57 477	K2.5IIIb CN1	1.606 ± 0.006	5.270	–	–	2.531 ± 0.060	12
59 746	K2III	1.498 ± 0.028	5.720	–	–	2.921 ± 0.080	12
60 202	K0III	1.651 ± 0.016	4.720	3.720 ± 0.027	–	2.321 ± 0.051	15
63 608	G8III	3.254 ± 0.037	2.850	1.970 ± 0.027	0.770 ± 0.050	0.731 ± 0.051	1, 2, 3
67 459	K5.5III	4.720 ± 0.050	4.050	2.440 ± 0.027	–	0.391 ± 0.041	3
68 594	G8:III: Fe-5	0.948 ± 0.012	6.180	–	3.775 ± 0.050	3.666 ± 0.015	16
69 673	K0III CH-1 CN-0.5	20.877 ± 0.277	–0.050	–1.330 ± 0.027	–2.951 ± 0.050	–	1, 11, 17, 18, 19
72 607	K4- III	10.300 ± 0.100	2.070	0.590 ± 0.027	–	–1.259 ± 0.070	1
74 666	G8IV	2.744 ± 0.036	3.460	2.480 ± 0.027	1.260 ± 0.050	1.121 ± 0.031	1, 2, 3, 6
74 793	K4III	2.336 ± 0.020	5.020	–	–	1.901 ± 0.051	12
75 260	K4III	1.690 ± 0.031	5.720	–	–	2.721 ± 0.060	12
75 458	K2III	3.596 ± 0.015	3.290	2.200 ± 0.027	–	0.701 ± 0.041	20
77 070	K2III	4.828 ± 0.062	2.630	1.560 ± 0.027	0.197 ± 0.007	0.041 ± 0.051	1, 2
79 882	G9.5IIIb Fe-0.5	2.961 ± 0.007	3.230	2.290 ± 0.027	–	0.961 ± 0.051	21
80 331	G8III-IV	3.633 ± 0.066	2.730	1.890 ± 0.027	–	0.601 ± 0.031	1, 2
80 816	G7IIIa Fe-0.5	3.492 ± 0.050	2.780	1.880 ± 0.027	0.690 ± 0.050	0.621 ± 0.041	1, 2
81 833	G7III Fe-1	2.529 ± 0.050	3.480	2.580 ± 0.027	–	1.281 ± 0.031	1, 2, 3
82 611	K2III	1.440 ± 0.004	5.990	–	–	2.811 ± 0.090	12
86 182	K1III	1.515 ± 0.010	5.350	–	–	2.651 ± 0.070	12
87 833	K5III	9.978 ± 0.180	2.240	0.630 ± 0.027	–1.160 ± 0.050	–1.319 ± 0.041	1, 11, 13, 17
90 344	K1.5III Fe-1	2.120 ± 0.020	4.820	3.630 ± 0.027	–	1.931 ± 0.051	22
93 194	A1III	0.753 ± 0.009	3.250	3.260 ± 0.027	3.195 ± 0.050	–	23
94 376	G9III	3.268 ± 0.054	3.070	2.120 ± 0.027	–	0.741 ± 0.051	1, 2
96 837	K0III	1.765 ± 0.012	4.390	3.410 ± 0.027	2.210 ± 0.050	2.071 ± 0.060	9
97 938	G9.5IIIb	1.726 ± 0.008	4.710	3.630 ± 0.027	–	2.351 ± 0.090	24
98 337	M0- III	6.821 ± 0.098	3.510	1.790 ± 0.027	–0.042 ± 0.050	–0.309 ± 0.041	1, 13, 25
99 663	K5III	1.859 ± 0.003	5.810	–	–	2.311 ± 0.070	12
102 488	K0III-IV	4.610 ± 0.050	2.480	1.450 ± 0.027	0.206 ± 0.050	0.101 ± 0.070	1
104 732	G8+ IIIa Ba0.5	2.820 ± 0.030	3.210	2.270 ± 0.027	1.155 ± 0.050	1.051 ± 0.031	1
110 538	G9IIIb Ca1	1.920 ± 0.020	4.420	3.400 ± 0.027	2.217 ± 0.050	1.961 ± 0.051	3
111 944	K2.5III	2.731 ± 0.024	4.500	3.190 ± 0.027	1.600 ± 0.007	1.391 ± 0.070	12

Angular Diameter References: (1) Mozurkewich et al. (2003); (2) Nordgren et al. (2001); (3) Nordgren et al. (1999); (4) Mozurkewich et al. (1991); (5) Boyajian (2009); (6) van Belle (1999); (7) Richichi & Roccatagliata (2005); (8) White & Feierman (1987); (9) van Belle et al. (2009); (10) Shao et al. (1988); (11) di Benedetto (1993); (12) Baines et al. (2010); (13) Hutter et al. (1989); (14) Thévenin et al. (2005); (15) von Braun et al. (2014); (16) Crepp et al. (2012); (17) Dyck et al. (1996); (18) Quirrenbach et al. (1996); (19) di Benedetto & Foy (1986); (20) Baines et al. (2011); (21) Mazumdar et al. (2009); (22) Ligi et al. (2012); (23) Maestro et al. (2013); (24) Baines et al. (2009); (25) Wittkowski et al. (2001). **Colour Magnitude References:** Neugebauer & Leighton (1969); Gezari et al. (1999); Carpenter (2001); Kidger & Martín-Luis (2003); Kimeswenger et al. (2004); Koen et al. (2010) and Mallama (2014); see Section 2 for more details.

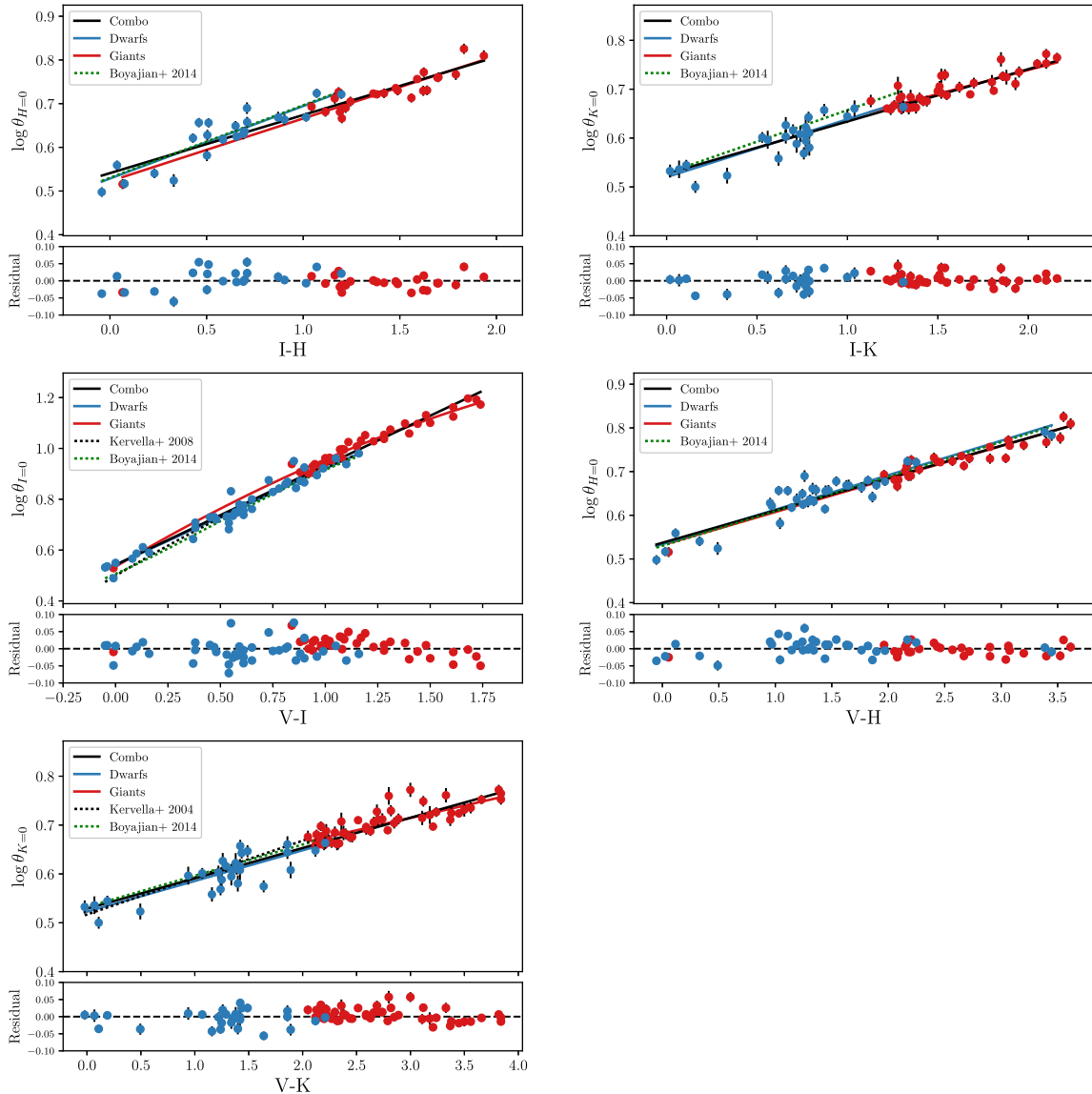


Figure 1. Top panels: Angular diameter–colour relations for both dwarf/subgiants (blue line) and giants (red line), as well as a combined fit (black line). The functional form of the fits is described in equation (3) with coefficients listed in Table 3. The data are introduced in Section 2 and catalogued in Tables 1 and 2. The fitting methodology is described in Section 4. All panels show previous relations from Boyajian et al. (2014). For $V - I_C$, we include the result for dwarfs from Kervella & Fouqué (2008), and for $V - K$ we include the result for dwarfs from Kervella et al. (2004b). Bottom panels: The residuals in dex are shown with respect to the combined relation.

of colours and fit coefficients for each fit. These relations are only valid for the colour ranges for which we have data. We then construct fits for each colour using all stars, unevolved and evolved. The combined fits test that variations in surface gravity with stellar evolution will not affect the relations (as noted in Section 1). The derived relations with the combined sample have similar root mean square (RMS) errors to the separated fits, which is consistent with the result of Barnes & Evans (1976) that surface brightness is independent of luminosity class. The RMS in the residuals ranges from 0.017 to 0.03 dex, corresponding to the minimum expected uncertainties in $\log \theta_{LD}$ before uncertainties in magnitudes are considered. The $I_C - K$ relations have the smallest spread for all fits.

To estimate the uncertainties in limb-darkened diameters, we propagate uncertainties for assumed 0.03 errors in both magnitudes of a given colour. The most precise relations for all stars

are those for $V - H$ and $V - K$, which have estimated uncertainties of 1.8–2.9 per cent. (The range is due to the dependence of the uncertainty on the colour, which we have varied within the range of the sample.) The least precise results are in $V - I_C$, where the corresponding uncertainties could be as high as 6.5 per cent.

Initially, M dwarfs were included in our sample to see if the derived relation would change drastically with their inclusion. The addition of dwarfs at $T < 3900$ K adds a statistically significant quadratic coefficient to our fits in the $V - I_C$ relation. Our temperature cut therefore provides a more precise relation for FGK stars in particular. In contrast, the $V - I_C$ relation in giants has a marginally significant quadratic term, even excluding stars below 3900 K. On the other end of our temperature range, inclusion of the A dwarfs (and one A giant) did not significantly change the fits, and so we are less hesitant to include them here.

Table 3. Angular diameter–colour relations.

Colour	N	Range	c_0	c_1	c_2	RMS (dex)	Pred. frac. uncertainty
All Stars							
$I_C - H$	47	−0.042–1.935	0.541 ± 0.004	0.133 ± 0.003	–	0.025	0.021–0.031
$I_C - K$	60	0.019–2.159	0.528 ± 0.005	0.108 ± 0.003	–	0.020	0.021–0.031
$V - I_C$	83	−0.050–1.740	0.542 ± 0.006	0.391 ± 0.006	–	0.028	0.043–0.065
$V - H$	63	−0.052–3.615	0.538 ± 0.004	0.074 ± 0.002	–	0.020	0.018–0.029
$V - K$	78	−0.021–3.839	0.529 ± 0.004	0.062 ± 0.002	–	0.021	0.018–0.029
Dwarfs and Subgiants							
$I_C - H$	22	−0.042–1.198	0.529 ± 0.007	0.166 ± 0.010	–	0.031	0.026–0.049
$I_C - K$	24	0.019–1.309	0.520 ± 0.007	0.118 ± 0.010	–	0.023	0.024–0.047
$V - I_C$	45	−0.050–1.160	0.542 ± 0.007	0.378 ± 0.011	–	0.029	0.043–0.070
$V - H$	35	−0.052–3.447	0.534 ± 0.005	0.079 ± 0.003	–	0.023	0.020–0.036
$V - K$	29	−0.021–2.209	0.523 ± 0.006	0.063 ± 0.005	–	0.024	0.022–0.038
Giants							
$I_C - H$	25	0.065–1.935	0.523 ± 0.011	0.144 ± 0.007	–	0.020	0.033–0.054
$I_C - K$	36	1.129–2.159	0.543 ± 0.011	0.098 ± 0.007	–	0.016	0.040–0.053
$V - I_C$	38	−0.010–1.740	0.535 ± 0.027	0.490 ± 0.046	-0.068 ± 0.019	0.026	0.080–0.241
$V - H$	28	0.055–3.615	0.532 ± 0.009	0.076 ± 0.003	–	0.016	0.026–0.041
$V - K$	49	2.049–3.839	0.562 ± 0.009	0.051 ± 0.003	–	0.019	0.031–0.040

Numerical values for the relations in Fig. 1. The colour index, number of stars per index, range of colour and fit coefficients for equation (3) (which takes the form $\log \theta_{Q=0} = \sum_{n=0}^N c_n (P - Q)^n$) are shown. For each relation, we have calculated both the RMS of the relation and the range of propagated fractional uncertainties for each zero-magnitude angular diameter, assuming 0.03 mag errors in each band.

We also test whether the angular diameter relations have a statistically significant dependence on stellar metallicity. Metallicity has shown to be a factor in relations of stellar radii to colour indices (Boyajian et al. 2012b), since changes in metallicity tend to affect bluer parts of the stellar spectra due to line blanketing (McNamara & Colton 1969). Such effects would propagate to stellar angular diameter relations, but in all colours considered in this paper the relations were insensitive to metallicity. This is consistent with the findings of Boyajian et al. (2014), who found that metallicity in their angular diameter relations was strongest for the colours with the shortest wavelength bands ($B - V$ and $g - r$), where the bluer colours would be affected more strongly by line blanketing.

4.1 Comparison with previous works

We directly compare our relations to those of Boyajian et al. (2014), and for $V - I_C$ to the relation in table 3 of Kervella & Fouqué (2008), and the $V - K$ relation to equation (23) of Kervella et al. (2004b), as seen in Fig. 1. All the mentioned relations are valid for dwarfs and subgiants, and it should be noted that all extend through the M spectral type (not shown here). In $V - I_C$, the largest offset in angular diameter between the data and the Kervella & Fouqué (2008) prediction is 0.08 dex, and for $V - K$ the largest offset with respect to Kervella et al. (2004b) is 0.06 dex. We expect at least a reasonable agreement with the results of Boyajian et al. (2014) and Kervella & Fouqué (2008) (see Fig. 1) by construct, since we include the subset of angular diameters used in these works which meet our uncertainty constraint (≤ 2 per cent). Nevertheless, our sources differ from these works for I_C (Koen et al. 2010; Mallama 2014), H (Gezari et al. 1999) and K (Neugebauer & Leighton 1969; Kidger & Martín-Luis 2003; Kimeswenger et al. 2004) band photometry, as well as a larger sample within the FGK colour range. Hence, differences in the predicted angular diameters exist, particularly on the blue end of the $V - I_C$ relation, where both Kervella & Fouqué (2008) and Boyajian et al. (2014) use higher-order polynomial fits which underestimate the diameters of the bluest dwarfs, while fitting well for dwarfs well beyond the red end of our colour range.

5 CONCLUSIONS

This work describes new relations linking stellar angular diameter to photometric colours. We use a data set with roughly twice the precision in angular diameter measurements compared to previous papers. We use empirical evidence that predictions of angular diameters from colour and magnitude are insensitive to luminosity class to construct, for the first time, a prediction of angular diameters at fixed magnitude for A–K stars across the stages of stellar evolution. We find that there is no dependence on stellar metallicity for the colours tested.

Further improvement to the relations will require additional angular diameter measurements to fill in parameter space for the earlier-type giants. Additionally, the lack of demonstrably consistent I_C photometry for M stars of any luminosity class limits us from extending the red end of our relations. Transformations among systems are susceptible to differences in zero-points, susceptibility of filters to red leaks and correlated errors in the filter profiles (Mann & von Braun 2015). Nevertheless, for FGK stars the continuity in the relation between colour and angular size is well constrained by the regions of overlap of the spectral classes.

ACKNOWLEDGEMENTS

This work was supported by a graduate fellowship from the Gruber Foundation. Additional gratitude to Anthony Mallama for providing converted Cousins I magnitudes for the dwarfs in our sample.

This research has made use of the NASA Exoplanet Archive, which is operated by the California Institute of Technology, under contract with the National Aeronautics and Space Administration under the Exoplanet Exploration Program.

REFERENCES

- Aufdenberg J. P. et al., 2006, *ApJ*, 645, 664
 Baines E. K., McAlister H. A., ten Brummelaar T. A., Turner N. H., Sturmann J., Sturmann L., Goldfinger P. J., Ridgway S. T., 2008, *ApJ*, 680, 728
 Baines E. K., McAlister H. A., ten Brummelaar T. A., Sturmann J., Sturmann L., Turner N. H., Ridgway S. T., 2009, *ApJ*, 701, 154

- Baines E. K. et al., 2010, *ApJ*, 710, 1365
 Baines E. K. et al., 2011, *ApJ*, 731, 132
 Barnes T. G., Evans D. S., 1976, *MNRAS*, 174, 489
 Boyajian T. S., 2009, PhD thesis, Georgia State University
 Boyajian T. S. et al., 2008, *ApJ*, 683, 424
 Boyajian T. S. et al., 2012a, *ApJ*, 746, 101
 Boyajian T. S. et al., 2012b, *ApJ*, 757, 112
 Boyajian T. S. et al., 2013, *ApJ*, 771, 40
 Boyajian T. S., van Belle G., von Braun K., 2014, *AJ*, 147, 47
 Boyajian T. et al., 2015, *MNRAS*, 447, 846
 Calchi Novati S. et al., 2010, *ApJ*, 717, 987
 Carpenter J. M., 2001, *AJ*, 121, 2851
 Chiavassa A., Bigot L., Kervella P., Matter A., Lopez B., Collet R., Magic Z., Asplund M., 2012, *A&A*, 540, A5
 Ciardi D. R., van Belle G. T., Akeson R. L., Thompson R. R., Lada E. A., Howell S. B., 2001, *ApJ*, 559, 1147
 Crepp J. R. et al., 2012, *ApJ*, 751, 97
 Cutri R. M. et al., 2003, *The 2MASS All Sky Catalog of Point Sources*. Pasadena: IPAC
 Davis J., Tango W. J., 1986, *Nature*, 323, 234
 Davis J., Ireland M. J., North J. R., Robertson J. G., Tango W. J., Tuthill P. G., 2011, *Publ. Astron. Soc. Aust.*, 28, 58
 Demory B. et al., 2009, *A&A*, 505, 205
 di Benedetto G. P., 1993, *A&A*, 270, 315
 Di Benedetto G. P., 2005, *MNRAS*, 357, 174
 di Benedetto G. P., Foy R., 1986, *A&A*, 166, 204
 Di Folco E., Thévenin F., Kervella P., Domiciano de Souza A., Coudé du Foresto V., Ségransan D., Morel P., 2004, *A&A*, 426, 601
 di Folco E. et al., 2007, *A&A*, 475, 243
 Dyck H. M., Benson J. A., van Belle G. T., Ridgway S. T., 1996, *AJ*, 111, 1705
 Fukui A. et al., 2015, *ApJ*, 809, 74
 Gezari D. Y., Pitts P. S., Schmitz M., 1999, *VizieR Online Data Catalog*, 2225, 0
 Hanbury B. R. H., Davis J., Lake R. J. W., Thompson R. J., 1974, *MNRAS*, 167, 475
 Hutter D. J. et al., 1989, *ApJ*, 340, 1103
 Iyengar K. V. K., Strafella F., Lorenzetti D., Cosmovici C. B., 1982, *JA&A*, 3, 451
 Kervella P., Fouqué P., 2008, *A&A*, 491, 855
 Kervella P., Thévenin F., Morel P., Bordé P., Di Folco E., 2003, *A&A*, 408, 681
 Kervella P. et al., 2004a, in Dupree A. K., Benz A. O., eds, *IAU Symp. 219, Stars as Suns: Activity, Evolution and Planets*. Astron. Soc. Pac., San Francisco, CA, p. 80
 Kervella P., Thévenin F., Di Folco E., Ségransan D., 2004b, *A&A*, 426, 297
 Kidger M. R., Martín-Luis F., 2003, *AJ*, 125, 3311
 Kimeswenger S. et al., 2004, *A&A*, 413, 1037
 Koen C., Kilkenny D., van Wyk F., Marang F., 2010, *MNRAS*, 403, 1949
 Koornneef J., 1983, *A&A*, 51, 489
 Ligi R. et al., 2012, *A&A*, 545, A5
 Maestro V. et al., 2013, *MNRAS*, 434, 1321
 Mallama A., 2014, *J. Am. Assoc. Var. Star Obs.*, 42, 443
 Mann A. W., von Braun K., 2015, *PASP*, 127, 102
 Markwardt C. B., 2009, in Bohlender D. A., Durand D., Dowler P., eds, *ASP Conf. Ser. Vol. 411, Astronomical Data Analysis Software and Systems XVIII*. Astron. Soc. Pac., San Francisco, p. 251
 Mazumdar A. et al., 2009, *A&A*, 503, 521
 McNamara D. H., Colton D. J., 1969, *PASP*, 81, 826
 Monnier J. D. et al., 2012, *ApJ*, 761, L3
 Mozurkewich D. et al., 1991, *AJ*, 101, 2207
 Mozurkewich D. et al., 2003, *AJ*, 126, 2502
 Neugebauer G., Leighton R. B., 1969, *Two-Micron Sky Survey. A Preliminary Catalogue*. NASA SP, NASA, Washington
 Nordgren T. E. et al., 1999, *AJ*, 118, 3032
 Nordgren T. E., Sudol J. J., Mozurkewich D., 2001, *AJ*, 122, 2707
 Press W. H., Teukolsky S. A., Vetterling W. T., Flannery B. P., 1992, *Numerical recipes in C. The art of scientific computing*, 2nd edn. Cambridge Univ. Press, Cambridge
 Quirrenbach A., Mozurkewich D., Buscher D. F., Hummel C. A., Armstrong J. T., 1996, *A&A*, 312, 160
 Richichi A., Roccatagliata V., 2005, *A&A*, 433, 305
 Shao M. et al., 1988, *ApJ*, 327, 905
 Thévenin F., Kervella P., Pichon B., Morel P., di Folco E., Lebreton Y., 2005, *A&A*, 436, 253
 van Belle G. T., 1999, *PASP*, 111, 1515
 van Belle G. T., Creech-Eakman M. J., Hart A., 2009, *MNRAS*, 394, 1925
 van Leeuwen F., 2007, *A&A*, 474, 653
 von Braun K. et al., 2011, *ApJ*, 740, 49
 von Braun K. et al., 2014, *MNRAS*, 438, 2413
 Wesselink A. J., 1969, *MNRAS*, 144, 297
 White N. M., Feierman B. H., 1987, *AJ*, 94, 751
 Wittkowski M., Hummel C. A., Johnston K. J., Mozurkewich D., Hajian A. R., White N. M., 2001, *A&A*, 377, 981

This paper has been typeset from a $\text{\TeX}/\text{\LaTeX}$ file prepared by the author.